Earth and Planetary Science Letters 462 (2017) 110–121

Contents lists available at ScienceDirect

Earth and Planetary Science Letters

www.elsevier.com/locate/epsl

Hydrothermal cooling of the ocean crust: Insights from ODP Hole 1256D

Michelle Harris [a,b,*], Rosalind M. Coggon [a], Martin Wood [a], Christopher E. Smith-Duque [a], Timothy J. Henstock [a], Damon A.H. Teagle [a]

[a] Ocean and Earth Science, National Oceanography Centre Southampton, University of Southampton, European Way, Southampton, SO14 3ZH, UK
[b] School of Geography, Earth and Environmental Sciences, Plymouth University, Plymouth, PL4 8AA, UK

ARTICLE INFO

Article history:
Received 13 July 2016
Received in revised form 21 December 2016
Accepted 11 January 2017
Available online 30 January 2017
Editor: M. Bickle

Keywords:
ocean crust
hydrothermal
Sr isotopes
heat flux

ABSTRACT

The formation of new ocean crust at mid-ocean ridges is a fundamental component of the plate tectonic cycle and involves substantial transfer of heat and mass from the mantle. Hydrothermal circulation at mid-ocean ridges is critical for the advection of latent and sensible heat from the lower crust to enable the solidification of ocean crust near to the ridge axis. The sheeted dike complex (SDC) is the critical region between the eruptive lavas and the gabbros through which seawater-derived recharge fluids must transit to exchange heat with the magma chambers that form the lower ocean crust.

ODP Hole 1256D in the eastern equatorial Pacific Ocean provides the only continuous sampling of in-situ intact upper ocean crust formed at a fast spreading rate, through the SDC into the dike–gabbro transition zone. Here we exploit a high sample density profile of the Sr-isotopic composition of Hole 1256D to quantify the time-integrated hydrothermal recharge fluid flux through the SDC. Assuming kinetically limited fluid–rock Sr exchange, a fluid flux of 1.5–3.2 $\times 10^6$ kg m^{-2} is required to produce the observed Sr-isotopic shifts. Despite significant differences in the distribution and intensity of hydrothermal alteration and fluid/rock Sr-isotopic exchange between Hole 1256D and SDC sampled in other oceanic environments (ODP Hole 504B, Hess Deep and Pito Deep), the estimated recharge fluid fluxes at all sites are similar, suggesting that the heat flux extracted by the upper crustal axial hydrothermal system is relatively uniform at intermediate to fast spreading rates.

The hydrothermal heat flux removed by fluid flow through the SDCs, is sufficient to remove only ~20 to 60% of the available latent and sensible heat from the lower crust. Consequently, there must be additional thermal and chemical fluid–rock exchange deeper in the crust, at least of comparable size to the upper crustal hydrothermal system. Two scenarios are proposed for the potential geometry of this deeper hydrothermal system. The first requires the downward expansion of the upper crustal hydrothermal system ~800 m into the lower crust in response to a downward migrating conductive boundary layer. The second scenario invokes a separate hydrothermal system in the lower crust for which fluid recharge bypasses reaction with the sheeted dikes, perhaps via flow down faults.

1. Introduction

Hydrothermal circulation is a key process in the formation and evolution of the ocean crust and impacts the broader Earth system through the modification of seawater chemistry and the subduction of altered ocean crust (Kelemen and Manning, 2015; Palmer and Edmond, 1989). At the ridge axis, hydrothermal circulation is intimately involved in the magmatic accretion of new crust through the advection of sensible and latent heat (e.g., Kelemen et al., 1997). Knowledge of the hydrothermal fluid fluxes and pathways through the crust are crucial to understanding the size, shape and distribution of magma bodies, and the processes of magma emplacement during the accretion of the ocean crust in the axial region.

The deficit between the predicted and observed conductive heat flow across the ocean basins persists on average until 65 ± 10 Ma, and implicates the cooling of the ocean crust by hydrothermal circulation. However, ~30% of the hydrothermal heat flux is advected from crust less than 1 million years old (Stein and Stein, 1994). In the axial region the magmatic heat released during the formation of the lower crust drives high-temperature (up to ~400 °C)

* Corresponding author at: School of Geography, Earth and Environmental Sciences, Plymouth University, Plymouth, PL4 8AA, UK.
E-mail address: michelle.harris@plymouth.ac.uk (M. Harris).

http://dx.doi.org/10.1016/j.epsl.2017.01.010

hydrothermal circulation, which manifests at the seafloor as black-smoker vents, and transports large heat and chemical fluxes to the oceans. Observations of the lower ocean crust by remote geophysical methods and drilling, and from tectonic windows and ophiolites have been essential in developing our understanding of the subsurface fluid/rock reactions and fluid pathways during hydrothermal circulation. However, long-standing questions remain about how the lower crust is cooled.

The axial high temperature fluid flux is recorded in the subsurface through the fluid/rock reactions within the sheeted dike complex that form secondary minerals, either in fractures or replacing primary igneous minerals. The sheeted dike complex has been sampled in four locations from in-situ ocean crust formed at intermediate to fast spreading rates: ODP Holes 504B and 1256D, and in the tectonic windows of Hess Deep and Pito Deep (Alt et al., 1996; Barker et al., 2008; Gillis et al., 2005; Wilson et al., 2006). ODP Holes 504B and 1256D sample intact ocean crust, providing continuous sections through the overlying volcanic sequences and the sheeted dikes, whereas at Hess and Pito Deep, local triple junction-related tectonics expose the deeper levels of the upper and lower crust at the seafloor. These contrasting methods of sampling the sheeted dikes yield differing perspectives. Drill cores enable high resolution vertical sampling that is complemented by the two dimensional but discontinuous sampling afforded in tectonic windows.

The relationship between the upper crustal hydrothermal system in the lavas and dikes, and the accretion of the lower oceanic crust remains poorly constrained, despite this zone being significant for the exchange of heat. Two end member models for the accretion of the lower oceanic crust have been proposed; the gabbro glacier (Henstock et al., 1993; Phipps Morgan and Chen, 1993; Quick and Denlinger, 1993) and the multiple sills models (Boudier et al., 1996; Kelemen et al., 1997; MacLeod and Yoauancq, 2000). These models have contrasting requirements for the magnitude and distribution of hydrothermal circulation to extract the latent and sensible heat released from the cooling and crystallisation of the lower crust. In the simplest, gabbro glacier, geometry the upper crustal hydrothermal system extracts much of the heat available from the lower crust, because all solidification occurs in a high-level magma chamber. In contrast, the multiple sills model requires deep hydrothermal heat advection to extract latent heat (Coogan et al., 2006). Hence, the thermal predictions of the models can be evaluated by quantifying the hydrothermal fluid flux through the sheeted dike complex that is driven by heat supplied from the lower crust.

Global hydrothermal fluid fluxes have been estimated directly through the extrapolation of modern vent fluxes (e.g., Baker et al., 1996) and indirectly from oceanic chemical budgets (e.g., Sr, Mg; Elderfield and Schultz, 1996; Palmer and Edmond, 1989) and the thermal balance of mid-ocean ridges (e.g., Morton and Sleep, 1985). Another approach is through the quantification of the total fluid/rock exchange that occurs between seawater and ocean crust during hydrothermal circulation using Sr isotopes as a tracer (Barker et al., 2008; Bickle and Teagle, 1992; Gillis et al., 2005; Teagle et al., 2003). The Hole 1256D and 504B whole rock $^{87}Sr/^{86}Sr$ profiles through the volcanic sequence and sheeted dike complex reveal clear differences in the distribution and intensity of Sr isotope exchange. Hole 1256D shows only limited seawater strontium exchange in the lavas but extensive isotopic re-equilibration in the sheeted dikes. In contrast, Hole 504B exhibits significant exchange in the lavas, but only slight $^{87}Sr/^{86}Sr$ increases in most of the dike section (Harris et al., 2015). These profiles may reflect significant differences in the timing and intensity of hydrothermal alteration and affect the global seawater–basalt exchange fluxes calculated for some elements.

In this paper we will investigate whether the contrasting extent of Sr-isotopic exchange in the sheeted dikes reflects different amounts of hydrothermal fluid recharge. We use the high sample density Sr isotope profile of ODP Hole 1256D (Harris et al., 2015) as a record of seawater–basalt exchange during hydrothermal recharge, to calculate the time integrated fluid flux through the sheeted dike complex. This fluid flux is compared to those calculated from the sheeted dike complex in Hole 504B, Hess Deep and Pito Deep to evaluate previous suggestions that hydrothermal recharge fluxes are uniform in sheeted dike complexes formed at intermediate to fast spreading rates (Barker et al., 2008). Our fluid flux is then converted into a hydrothermal heat flux to evaluate the thermal budgets implied by contrasting models of ocean crust accretion.

2. Geological setting

ODP Hole 1256D is located in the eastern equatorial Pacific and is the only complete sampling of intact in-situ upper oceanic crust down to the dike/gabbro transition (Fig. 1; Teagle et al., 2006, 2012; Wilson et al., 2006). Site 1256 formed at the East Pacific Rise 15 myr-ago during an interval of superfast spreading (>200 mm/yr full rate; Wilson, 1996). The ocean crust at Site 1256 is covered by 250 m of sediments and Hole 1256D samples 750 m of extrusive volcanic rocks, a thin mineralized lava-dike transition, 350 m of sheeted dikes, and 120 m into the dike/gabbro transition where two thin gabbro sills are intruded into contact metamorphosed sheeted dikes (Teagle et al., 2006, 2012; Wilson et al., 2006).

The assemblages of secondary minerals document a downhole transition from low temperature phases (e.g., clays, oxyhydroxides, carbonates) in the volcanic sequence to greenschist facies phases (e.g., chlorite, actinolite, albite) in the sheeted dike complex (Alt et al., 2010). This alteration is broadly similar to the only other penetration of intact in-situ upper ocean crust drilled in Hole 504B (Alt et al., 1996). Studies of tectonic windows also record greenschist facies alteration in the sheeted dike complex, although at Pito Deep amphibole dominates the alteration assemblage (Heft et al., 2008) whereas at Hess Deep chlorite is more dominant (Gillis et al., 2005). Careful inspection of the Hole 1256D drill core and thin sections allows the classification of dike samples into: background alteration, alteration patches and vein halos, and dike margin categories. In the dike/gabbro transition early amphibole alteration is overprinted by granulite facies contact metamorphism and later lower temperature hydrothermal alteration at greenschist facies conditions and below (Alt et al., 2010).

The whole rock Sr isotope profile of Hole 1256D records the evolution of fluid pathways in the hydrothermal system and shows distinct variation between the main stratigraphic sequences (Fig. 1; Harris et al., 2015). The volcanic sequence has limited increases in $^{87}Sr/^{86}Sr$ except along brecciated horizons and the margins of anomalously thick massive flows. This suggests that the hydrothermal recharge fluid reaching the top of the sheeted dikes had undergone only minor modification from seawater $^{87}Sr/^{86}Sr$. Large increases in $^{87}Sr/^{86}Sr$ in the lava-dike transition are restricted to mineralized, brecciated horizons and reflect the sub-surface mixing of upwelling and downwelling fluids.

The sheeted dike complex provides pathways for both downwelling recharge fluids and upwelling hydrothermal discharge (Harris et al., 2015), and dikes display strongly elevated $^{87}Sr/^{86}Sr$ towards our estimated end member hydrothermal fluid composition, indicating extensive fluid/rock exchange at greenschist facies conditions (Fig. 1). The Sr-isotopic composition of the upwelling hydrothermal fluid is estimated from analyses of hydrothermal epidote ($n = 5$) that precipitated in veins and alteration patches. Epidote is selected as it has high Sr concentrations (>500 ppm) so is robust to overprinting, and it is commonly associated with

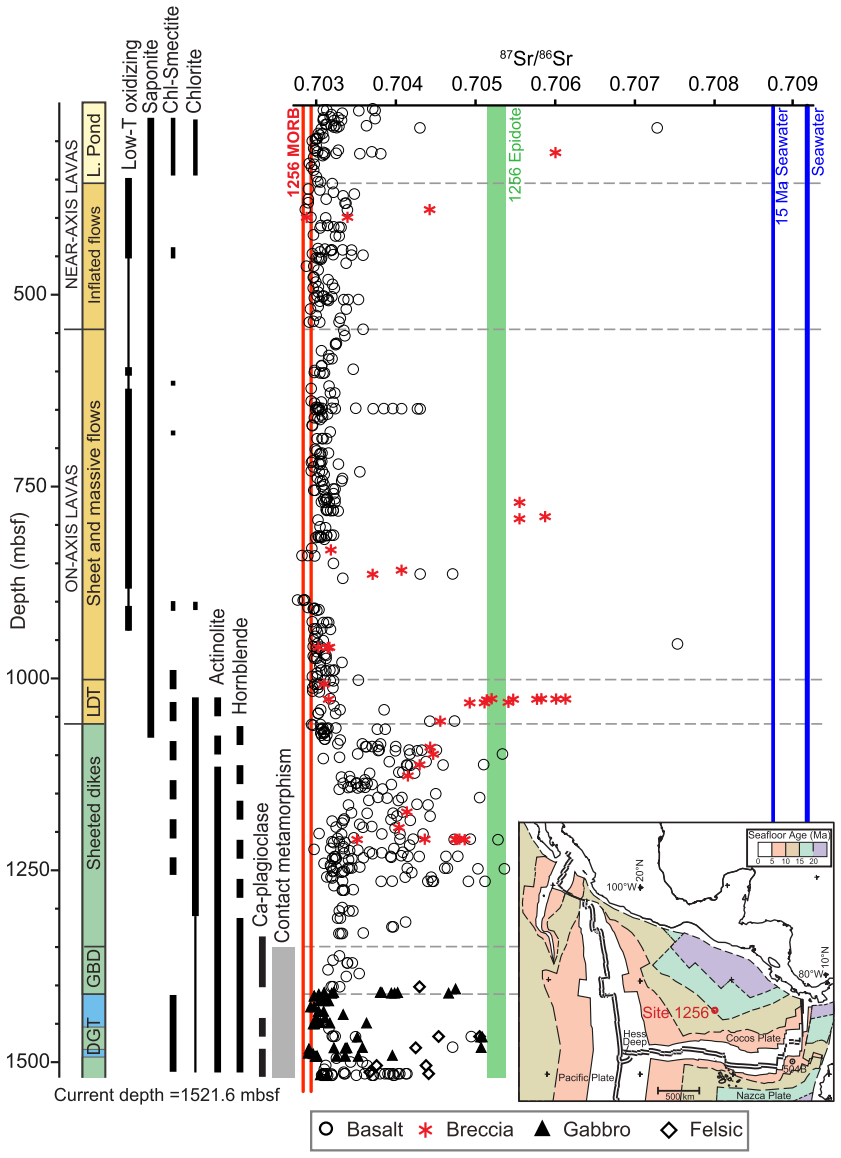

Fig. 1. Location of ODP Hole 1256D on a crustal age map (5 myr intervals) after Wilson et al. (2003) (inset) and whole rock Sr isotope profile through Hole 1256D, shown relative to fresh MORB, hydrothermal fluid end member, modern day seawater and 15 Ma seawater (modified from Harris et al., 2015).

subsurface black smoker-like mineralization (e.g., Bickle and Teagle, 1992). Crucially the five epidotes analysed, which were sampled from the sheeted dike complex and the dike–gabbro transition, record a very limited range of fluid Sr-isotopic compositions ($^{87}Sr/^{86}Sr_{EPIDOTE}$ = 0.70505–0.70525, Harris et al., 2015). Although the $^{87}Sr/^{86}Sr$ composition of these epidotes is higher than modern hydrothermal fluids sampled at intermediate to fast spreading rates ($^{87}Sr/^{86}Sr_{mean}$ ~0.7038; Bach and Humphris, 1999), the range is consistent with the extrapolation of the observed relationship between fluid composition and spreading rate to the superfast spreading rate of Site 1256 (200–220 mm/yr; Bach and Humphris, 1999). This approach predicts vent fluid $^{87}Sr/^{86}Sr$ of 0.7051–0.7056.

The dike margins generally record higher $^{87}Sr/^{86}Sr$ relative to dike cores, and provided preferential recharge and discharge fluid channels through the sheeted dike complex. Hydrothermal circulation through the dike complex is therefore spatially and temporally variable. The dike/gabbro transition is characterised by elevated $^{87}Sr/^{86}Sr$ along igneous contacts that were the loci for channelised fluid flow, although with only minor increases in $^{87}Sr/^{86}Sr$ in the interiors of the gabbro sills (Harris et al., 2015).

3. Method

Hydrothermally altered sections of ocean crust record the time-integrated effects of fluid–rock reaction. The extent of fluid/rock exchange can be used to quantify the magnitude of the time integrated fluid flux through the section, that is the total volume of fluid that passed through a unit area of crust. Here we model the time integrated fluid flux assuming one dimensional kinetically limited fluid–rock tracer exchange, following Bickle (1992), Bickle and Teagle (1992); see Supplementary Methods. This method uses the Damköhler number, the ratio of the advective tracer transport time to the perpendicular tracer exchange time, to describe the effectiveness of wall rock tracer exchange. The Simplex algorithm is used to fit the Damköhler number and fluid flux penetration distance to the Sr-isotopic composition of whole rock and epidote mineral analyses by minimising the root-mean-square error (Press et al., 1992). These models assume hydrothermal recharge occurs regionally via porous media flow or through very closely spaced fractures, whereas the upwelling black smoker fluids ascend through the sheeted dike complex via concentrated discharge zones (see Bickle and Teagle, 1992). We assume that exchange

Table 1
Parameters used in the Hole 1256D fluid flux models and heat flux calculations.

Parameter	Value	Reference
Initial rock $^{87}Sr/^{86}Sr$	0.7028	(Harris et al., 2015)
Initial rock [Sr] $= C_s$	79 ± 16 ppm	(Harris et al., 2015)
Initial fluid $^{87}Sr/^{86}Sr$	0.70875	(McArthur et al., 2001)
Initial fluid [Sr] $= C_f$	8 ppm	
Density of upper ocean crust (ρ_s)	2700 kg/m^3	
Density of fluid (ρ_f)	1000 kg/m^3	
Final fluid $^{87}Sr/^{86}Sr$	0.70505–0.70525	(Harris et al., 2015)
Volumetric solid/fluid partition coefficient: $K_v = \frac{\rho_f C_f}{\rho_s C_s}$	0.038	
Heat required to raise 1 kg of seawater from 0–440 °C	1.93×10^6 J/kg	(Driesner, 2007)
Thickness of lower crust at Site 1256	3.75–4.25 km	(Wilson et al., 2003)
Full spreading rate at Site 1256D	220 mm/yr	(Wilson et al., 2003)
Latent heat crystallisation	5.06×10^5 J/kg	(Kojitani and Akaogi, 1997)
Specific heat capacity gabbro	1085 J/kg/K	(Berman, 1998)

with the whole rock is limited only by the relative rate of kinetic exchange. The mass balance assumes that past seawater had the same Sr concentration as modern seawater (Table 1), and that, on average, the Sr content of the reacting fluid is little changed throughout the fluid flow pathway, as supported by the similar Sr concentrations of modern seawater and black smoker fluids ([Sr] = 65–257 µmol/kg, Von Damm, 1995). The epidote and rock data populations are given equal weighting in the model, regardless of their differing population sizes, to force the fluid to evolve to epidote compositions at the base of the model interval.

The different alteration/igneous features identified (pervasive background alteration, alteration patches and halos, dike margins) represent differences in pathways and extent of fluid–rock interactions (Harris et al., 2015). To investigate their potential contribution to the fluid flux through Hole 1256D, the best-fit fluid fluxes and Damköhler numbers are calculated for each category: background only, halos/patches, dike margins, as well as the complete dataset (Table 2).

The initial $^{87}Sr/^{86}Sr$ of the rock is the primary MORB composition (0.7028; Harris et al., 2015) and the final rock composition is the whole rock $^{87}Sr/^{86}Sr$ profile. Both the best fit to the entire dataset ($n = 196$), along with the best fit to 10 m averages are determined. Based on the minimal change in whole rock $^{87}Sr/^{86}Sr$ in the overlying volcanic sequence, the fluid entering the top of the sheeted dikes is interpreted to have a composition that is little changed from 15 Ma seawater ($^{87}Sr/^{86}Sr$ 0.70875; McArthur et al., 2001). The final fluid composition is represented by the estimated hydrothermal fluid composition for Hole 1256D, as determined by epidote mineral separates (0.70505–0.70525).

The modelled zone begins at the top of the sheeted dike complex (1060 m below seafloor) at the onset of greenschist facies alteration, and extends down to the dike/gabbro transition, with a total thickness of 390 m (Fig. 2). The latter is based on the assumption that the base of the black smoker hydrothermal system is a narrow conductive boundary layer (CBL) overlying a convecting magma chamber in the uppermost gabbros. This assumption is consistent with the observed contact metamorphism in the lowermost Hole 1256D sheeted dikes under granulite facies conditions (Teagle et al., 2006). Thermal calculations indicate that these 'granoblastic' dikes formed in a CBL overlying a steady state high-level axial magma chamber (Koepke et al., 2008), similar to previously documented CBL in the Troodos ophiolite (Gillis and Coogan, 2002). The modelled interval includes 350 m of sheeted dike complex and 40 m of granoblastic dike screens that were part of the dike complex and are now within the dike/gabbro transition. The granoblastic dikes have a narrow range of whole rock Sr isotopic compositions, which are interpreted to have been homogenised during recrystallisation to record an average $^{87}Sr/^{86}Sr$ composition created during hydrothermal circulation at the ridge axis (Harris et al., 2015). Late stage gabbroic intrusives and minor associated felsic rocks are excluded from our calculations.

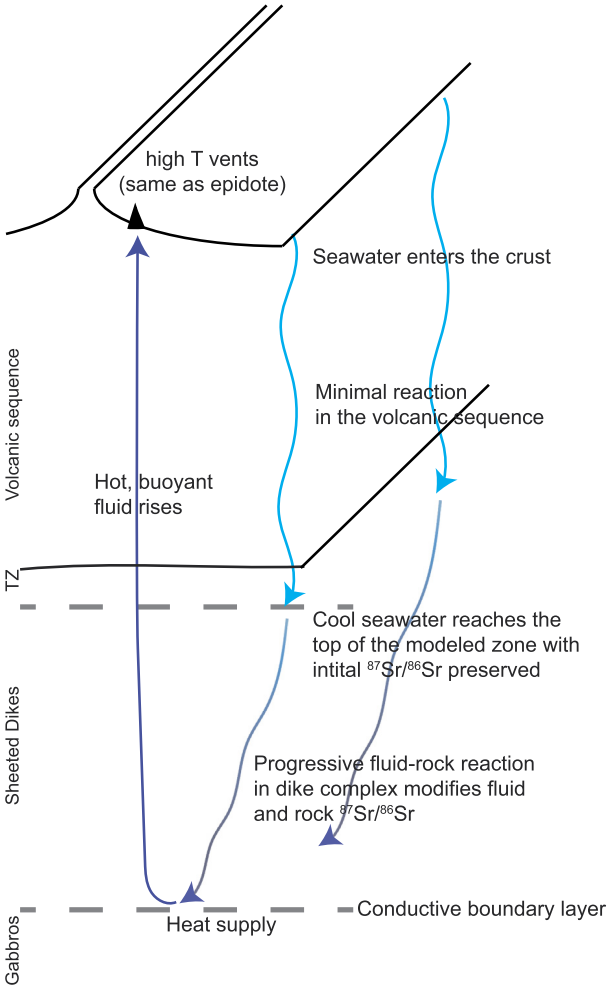

Fig. 2. Illustration of the set up for the tracer transport model used in this study, showing the assumed fluid flow path through the crust in different parts of the model.

4. Results

The best fit time-integrated fluid flux and Damköhler number for each modelled scenario for Hole 1256D are shown in Table 2. The difference between fitting the model to all data points and to 10 m downhole averages is minor (Fig. 3). A scenario including all the available data requires a minimum time integrated fluid flux of 2.2×10^6 kg m^{-2} with a N_D of 0.27 (Fig. 3). This Damköhler number indicates partial fluid–solid exchange and is consistent with the observed partial recrystallisation of the dikes to greenschist facies minerals. Our high sampling density allows us to evaluate the potential variability in the fluid flux and Damköhler number that are associated with the different alteration regimes ($1.5–3.2 \times 10^6$ kg m^{-2} and $N_D = 0.16–0.44$, respectively; Fig. 3; Table 2), confirming that although fluid/rock reaction is heterogeneous within the Hole 1256D sheeted dikes, variations are relatively minor.

Table 2
Time integrated fluid fluxes determined from Sr-isotopic exchange.

Location	Crustal age (Ma)	Full spreading rate (mm yr^{-1})	Model depth (m)	$^{87}Sr/^{86}Sr$ fluid[a]	K_v	Model results[b]		Literature values[c]	
						N_D	Fluid flux ($\times 10^6$ kg m^{-2})	N_D	Fluid flux ($\times 10^6$ kg m^{-2})
Hole 1256D all samples	15	220	390	0.70505–0.70525[d]	0.0375	0.25	2.2	–	–
Hole 1256D 10 m averages	15	220	390	0.70505–0.70525[d]	0.0375	0.27	2.3	–	–
Hole 1256D background samples only	15	220	390	0.70505–0.70525[d]	0.0375	0.16	1.5	–	–
Hole 1256D alteration halos & patches	15	220	390	0.70505–0.70525[d]	0.0375	0.32	2.6	–	–
Hole 1256D dike margins	15	220	390	0.70505–0.70525[d]	0.0375	0.44	3.2	–	–
Hole 504B	6.9	66	1035	0.7034–0.7038[e]	0.0476	0.19	2.2	0.2[f] 0.1[g]	1.7[f] 2.1[g]
Hess Deep	1	130	700	0.7038–0.7044[h]	0.0329	0.09	1.4	0.1[g]	1.5[g]
Pito Deep	3	142	1080	0.70382–0.70413[g]	0.0312	0.09	2.3	0.1[g]	2.4[g]

[a] Sr isotopic composition of end-member hydrothermal fluid, constrained by epidote Sr-isotope analyses;
[b] Time integrated fluid fluxes for Hole 1256D and recalculated from published Sr-isotopic profiles, allowing both N_D and fluid flux to vary by constraining the final fluid at the base of the system;
[c] Previously published time integrated fluid fluxes.
[d] Harris et al., 2015;
[e] Teagle et al., 1998;
[f] Teagle et al., 2003;
[g] Barker et al., 2008;
[h] Harris, unpublished data.

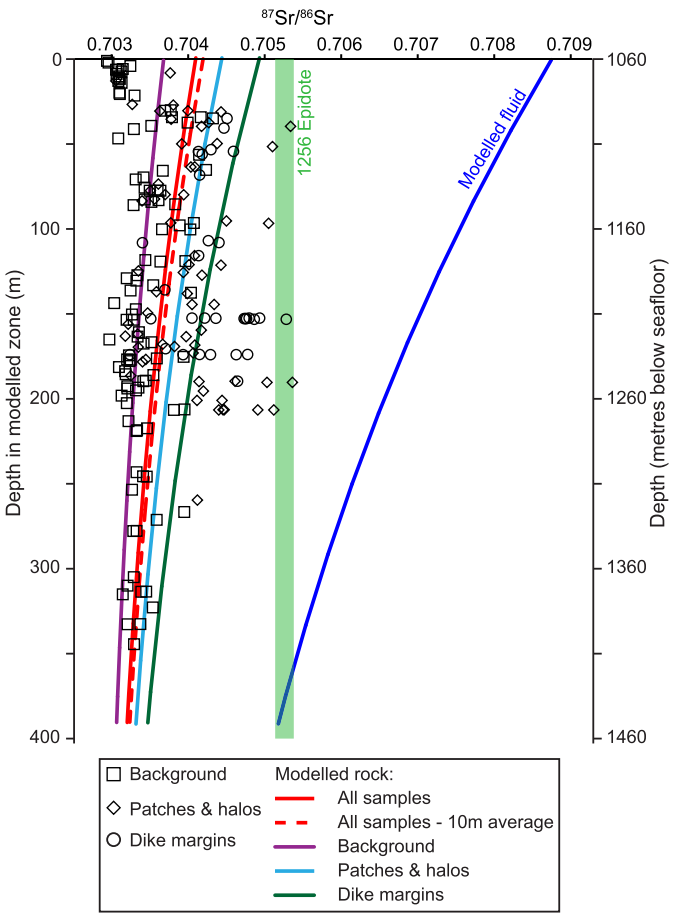

Fig. 3. Tracer transport results for Hole 1256D showing the modelled final rock and fluid compositions overlain on the whole rock Sr isotope profile. Separate curves are shown for background, patches and dike margins.

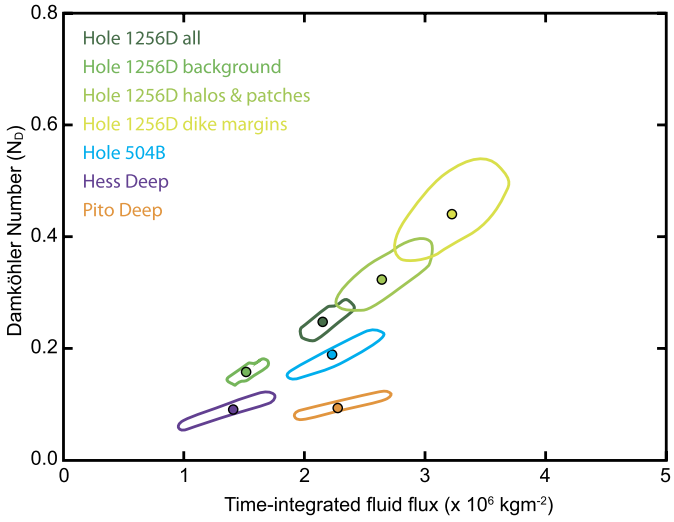

Fig. 4. Confidence region of the optimised solution based on the 2 parameters (N_D and time-integrated fluid flux) for each of the study sites. The optimal solution for each case is shown by a colour coded filled circle with the surrounding ellipse representing the 95% confidence region, and the potential range in both N_D and fluid flux that could be attained by the model.

In order to compare the results from Hole 1256D to other crustal sites in a self-consistent manner, the time integrated fluid fluxes for Hole 504B, Hess Deep and Pito Deep have been recalculated following the same approach (Table 2). The best-fit models for Hole 504B, Hess and Pito Deep have N_D 0.09–0.19, and time-integrated fluid fluxes of 1.4–2.2 $\times$ 10^6 kg m^{-2} (Table 2). These results are similar to those calculated using a constant N_D of 0.1 (Barker et al., 2008).

The 95% confidence interval for the optimal solution of the time-integrated fluid flux and N_D was calculated for each crustal site (Fig. 4) by performing an F-test for non-linear confidence intervals using the SSE for each solution. The confidence intervals demonstrate that the N_D is generally better constrained than the

time-integrated fluid flux. The confidence intervals for the time-integrated fluid flux are variable but always $<0.5 \times 10^6$ kg m^{-2}.

5. Discussion

5.1. Validity of assumptions

A key assumption of this mass balance approach is that Sr is immobile during hydrothermal alteration, which is supported by the similar Sr contents of seawater and black smoker fluids (Teagle et al., 2003) and experimental fluid–rock exchange experiments (Berndt et al., 1988). However, previous studies have suggested that Sr is mobile during hydrothermal circulation and it can be lost from either the fluid or the rock (Barker et al., 2008, 2010a). Sr can be lost from the fluid through the recrystallisation of igneous plagioclase, or through the precipitation of anhydrite, although this process remains poorly quantified (Teagle et al., 1998, 2003). The variation in Sr concentrations in the hydrothermally altered samples can be compared to the predicted igneous concentration to assess whether Sr has been mobilised during hydrothermal alteration. This is complicated by the insensitivity of Sr to magmatic fractionation (Coogan and Dosso, 2012) and for Hole 1256D the magmatic composition is best estimated from the least altered samples, which have Sr concentrations in the range 60–100 ppm (Harris et al., 2015). In the sheeted dike complex only a small proportion of the samples have undergone Sr loss (8%) or Sr gain (15%), with Sr mobility predominantly restricted to alteration patches or dike margins rather than the background samples. This suggests that although there can be local mobilisation of Sr, on average the bulk composition of the crust remains constant. In contrast, ~30% of background samples from Pito Deep have lost Sr (Barker et al., 2008) and a synthesis of global data indicates that black smoker fluids have elevated Sr concentrations compared to seawater (Coogan and Dosso, 2012). If the Hole 1256D dikes had undergone substantial pervasive Sr loss (>9 ppm) similar to Pito Deep, then this would result in a decrease in the time-integrated fluid flux by 0.5×10^6 kg m^{-2}. In contrast, the loss of Sr from the fluid due to the precipitation of anhydrite would increase the estimated fluid fluxes (Barker et al., 2008). In Hole 1256D anhydrite is present over several hundred metres and is most abundant in the lava-dike transition zone and the upper 200 m of the sheeted dike complex. It is more abundant than in Hole 504B, albeit only as a minor phase (Teagle et al., 2006). If the fluid lost 40% of its Sr through anhydrite precipitation (following Barker et al., 2008), the Hole 1256D fluid flux would increase by 1.2×10^6 kg m^{-2}.

The complex transition between the upper and lower crust has been observed at Hess Deep, Pito Deep and in the Troodos and Semail ophiolites (France et al., 2009; Gillis, 2008). Hole 1256D also shows a similar complexity of the upper-lower crust transition in terms of assimilation and the migration of the axial melt lens. Such migration results in uncertainty regarding the thickness of the sheeted dike complex and hence the thickness of the modelled zone, which is critical for calculating the fluid flux. A key result of the Hole 1256D drilling was the successful prediction of the upper crustal thickness (depth to gabbro) from the observed relationship between spreading rate and the depth to seismically imaged axial melt lenses (Wilson et al., 2006). Given the thickness of the volcanic sequence in Hole 1256D, the predicted upper crustal thickness equates to a sheeted dike thickness of 214–489 m. 390 m of sheeted dikes have now been cored in Hole 1256D. Increasing the model interval by 100 m to reflect the maximum predicted thickness of sheeted dikes increases the time-integrated fluid flux by $0.3–0.7 \times 10^6$ kg m^{-2}, where the range reflects the variable Sr-isotopic compositions of background and margin samples. The potential variability in the input parameters (Sr concentration, model depth) results in uncertainty in the calculated fluid flux of comparable magnitude to the model confidence intervals, and does not significantly impact interpretation of the fluid flux.

5.2. Ocean crust fluid fluxes

The four ocean crust sheeted dike complexes sampled to date differ primarily in their thickness, with the Hole 1256D sheeted dike complex being much thinner (~400 m v >1000 m) than at Hole 504B, Hess Deep and Pito Deep (Alt et al., 1996; Barker et al., 2008; Gillis et al., 2005; Wilson et al., 2006). The Sr isotope profiles for the sheeted dike complexes are also different. Given the nature of the sampling at the different sites, the samples from Hess and Pito Deep are most comparable to the 1256D background rocks. The $^{87}Sr/^{86}Sr$ profile through Hole 504B shows a decrease in strontium isotope composition with depth whereas the Pito and Hess Deep profiles are generally uniform with depth (Fig. 5). The Sr profile for the Hole 1256D dike complex records the greatest extent of fluid/rock exchange of all the profiles. This difference in Sr isotopes is highlighted by normalised cumulative frequency curves where the distribution for Hole 504B, Hess Deep and Pito is very similar for ~80% of the population (Fig. 5). However, the Hole 1256D cumulate frequency curve is markedly different to the other populations, even when the more altered dike margins are removed from the Hole 1256D population. The greater exchange in Sr isotopes in the dikes in Hole 1256D may result from the narrow thickness of the dike complex and the consequent steeper thermal gradient present, as reflected in the higher best fit Damköhler number. The range of the time-integrated fluid flux for the Hole 1256D sheeted dike complex ($1.5–3.2 \times 10^6$ kg m^{-2}) is comparable to estimates from other crustal locations, despite major differences in their whole rock Sr isotope profiles. This result therefore suggests that although the high temperature fluid flux of the axial hydrothermal system is comparable at intermediate to superfast spreading rates, the distribution and intensity of the associated hydrothermal alteration and the resultant chemical exchange varies between the studied crustal sections. This variability in Sr-isotope exchange is also apparent for the upper crustal volcanic sequences in Hole 1256D and Hole 504B (Harris et al., 2015) indicating there may be a disconnect between the axial recharge fluid flux and the crustal chemical budgets for certain elements, especially those exchanged at lower temperatures (e.g., C, Mg, Tl, K).

The axial high temperature hydrothermal fluid flux has been estimated using a variety of other geochemical tracers. Estimates based on thallium (Nielson et al., 2006) and sulphur budgets (Barker et al., 2010a; Teagle et al., 1998) of $2.4–3.0 \times 10^6$ kg m^{-2} are comparable to those calculated from Sr isotope tracer transport, whereas the estimate from lithium isotopes (Chan et al., 2002) shows a much greater range ($1.3–8.7 \times 10^6$ kg m^{-2}), but remains a similar order of magnitude (Fig. 6). In contrast, indirect estimates from global geochemical budgets (e.g., Sr Palmer and Edmond, 1989) are an order of magnitude larger, as are those estimated from the Troodos ophiolite (Bickle and Teagle, 1992).

From the limited crustal sections available, the estimated axial high temperature hydrothermal recharge fluid flux recorded by the dike rocks appears insensitive to spreading rate and differences in the relative thickness of the upper crust. The overall agreement between estimates of the axial high temperature fluid flux from a variety of tracers and multiple study sites, along with the comparability in the temperature of fluid/rock reactions, indicates a surprising uniformity of the hydrothermal system at intermediate to fast spreading rates, albeit with very limited sampling. This suggests that the total heat removed by axial hydrothermal circulation through the sheeted dikes is also fairly uniform and can therefore be used to investigate the thermal constraints of the end member models for the accretion of the ocean crust.

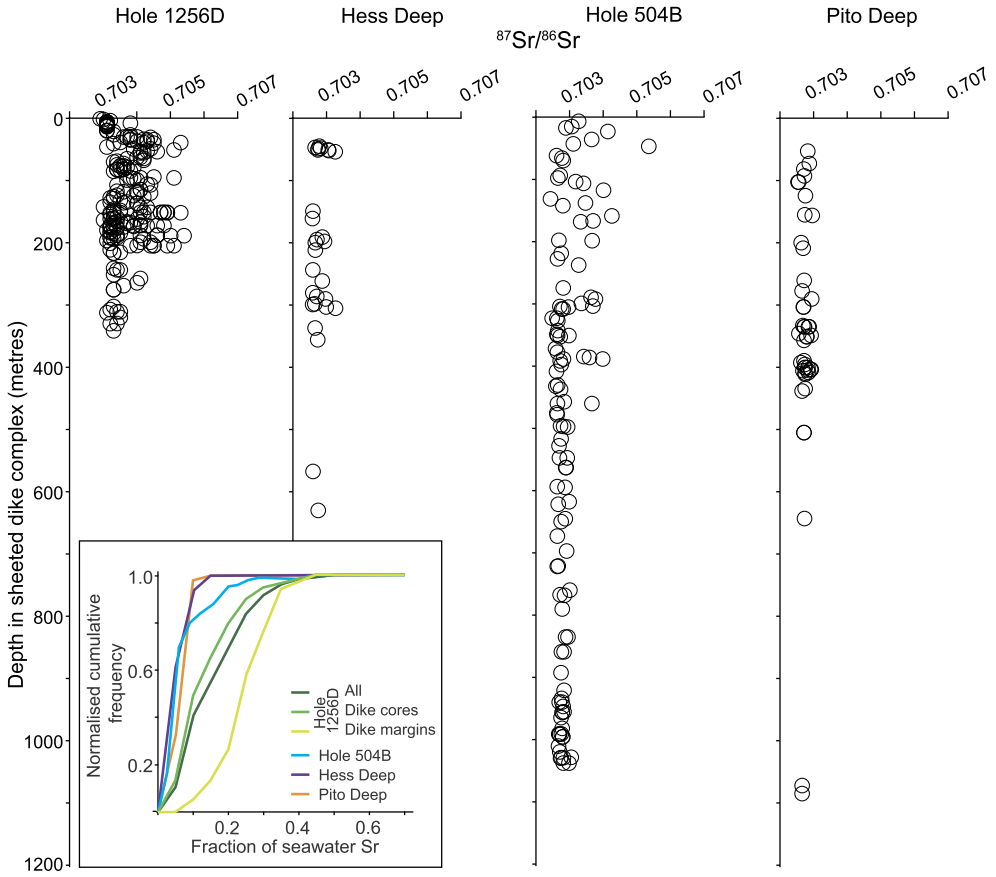

Fig. 5. Whole rock $^{87}Sr/^{86}Sr$ profiles of the sheeted dike complexes sampled at intermediate to fast spreading rate crust. See in-text discussion for data sources. Inset: cumulative frequency diagram for the extent of Sr isotope exchange in the sheeted dike complexes for Hole 1256D (all, cores and margins, where cores include background and patches), Hole 504B, Hess Deep and Pito Deep, where the fraction of seawater Sr is defined as: Fraction seawater Sr = ($^{87}Sr/^{86}Sr$ $Rock_{measured}$ − $^{87}Sr/^{86}Sr$ $Rock_{MORB}$)/($^{87}Sr/^{86}Sr$ SW_{Sr} − $^{87}Sr/^{86}Sr$ $Rock_{MORB}$).

Some models of axial hydrothermal circulation propose that most fluid/rock reactions within the sheeted dike complex occur during regional discharge (Coogan, 2008) and not recharge (Bickle and Teagle, 1992), based on modelling that shows that large fluxes of downwelling fluids cool the upper dikes too efficiently (Coogan, 2008; Teagle et al., 2003). Consequences of the Coogan (2008) model should be the transport of seawater signatures (e.g., K, Mg, O, ^{87}Sr) down to the base of the sheeted dike complex. In Hole 1256D, there is little change in Mg once magmatic fractionation is accounted for, and relatively light oxygen isotope compositions indicate hydrothermal exchange at high temperatures in the sheeted dikes (Gao et al., 2012). Similarly, the downhole variability in Fe^{3+}/Fe_{TOT} through the sheeted dike complex is also minimal (<15%) with no trend with depth (Rutter, 2015). B/K and Cl/K ratios from the dike complex are also consistent with high temperature alteration and do not record evidence of seawater (Sano et al., 2008). These profiles suggest that there is little evidence for cold seawater penetrating deep into the sheeted dike complex. The decrease in whole rock Sr isotopes with depth in the sheeted dike complex of Hole 1256D is consistent with reaction during recharge and not discharge.

At Pito Deep evidence of focussed fluid flow has been observed in 1 m intervals over a 40 m-wide fault-zone just below the lava-dike transition (Barker et al., 2010b). These fault-zones are sub-parallel to the dike margins and have Sr isotope compositions that are consistent with the mixing of upwelling hydrothermal fluids and downwelling seawater, similar to the brecciated horizons in the lava/dike transition in Hole 1256D. If the Pito Deep observations are more representative of typical intermediate to fast spreading rate crust, then hydrothermal circulation in the sheeted dikes may additionally occur via focussed pathways, although such zones are not strongly developed in Hole 1256D beyond the dike margins. Fluid fluxes modelled using the mass balance approach adopted here could therefore represent the minimum amount of fluid/rock reaction in the dike complex.

5.3. Ocean crust heat fluxes

To evaluate the proposed end-member crustal accretion models, we convert the calculated hydrothermal fluid flux into a hydrothermal heat flux and compare this to the heat available from the crystallisation and cooling of the sheeted dike complex and the lower ocean crust. In the following discussion we assume that no focussed fluid flow occurs in the dike complex, and consider the consequences of this for the lower crust.

5.3.1. Hydrothermal heat flux

The heat flux that is transported through a unit area of crust by hydrothermal fluids is given by:

$$Q_{ht} = F \int_{T_{sw}}^{T_{ht}} C_p . \mathrm{d}T \tag{1}$$

where: Q_{ht} is the hydrothermal heat flux ($J\,m^{-2}$); F is the hydrothermal fluid flux ($kg\,m^{-2}$); C_p is the specific heat capacity of the fluid ($J\,kg^{-1}\,{}^{\circ}C^{-1}$), which is a function of temperature (T) and pressure; and T_{sw} and T_{ht} are the temperatures of seawater and

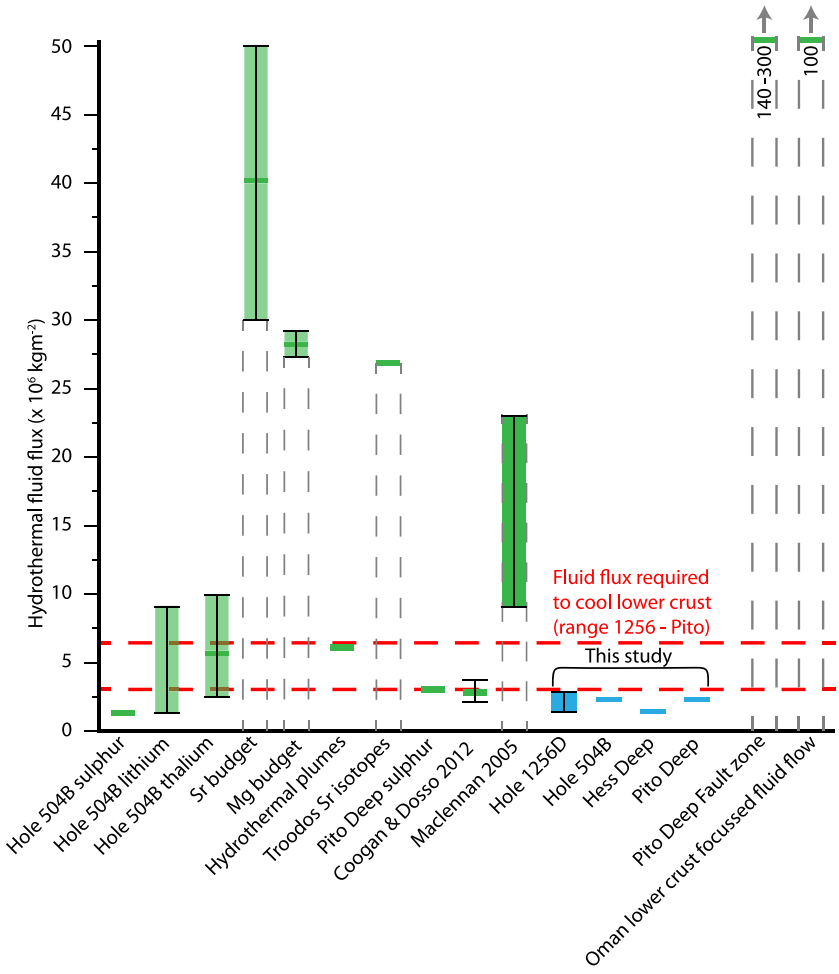

Fig. 6. Compilation of literature estimates for the high temperature axial hydrothermal fluid flux. For each estimate the range is represented by the error bar and lighter shaded region, and the solid bar represents either the preferred or mid-point of the range. Data and references presented in this figure are located in Supplementary Material Table 1.

the venting hydrothermal fluid, respectively. For simplicity we assume that all of the fluid flux is heated from 0 °C up to the critical point for seawater at the base of the dikes (440 °C at 40 MPa; Bischoff and Rosenbauer, 1985), consistent with maximum alteration temperatures and vent fluid temperatures (Alt et al., 2010; Von Damm, 1995). The energy required to heat 1 kg of seawater to 440 °C is 1.9×10^6 J kg^{-1} (Driesner, 2007). Given our best estimate of the axial high temperature hydrothermal fluid flux at Site 1256 ($1.5–3.2 \times 10^6$ kg m^{-2}), the associated hydrothermal heat flux, calculated using Equation (1), is $2.9–6.2 \times 10^{12}$ J m^{-2}.

5.3.2. Crustal accretion heat flux

The axial magmatic heat flux through a unit area of crust comprises both the latent heat of crystallisation and the sensible heat released during cooling, and is given by:

$$Q_{\text{magmatic}} = \rho h[L + C_p \Delta T] \quad (2)$$

where: Q_{magmatic} is the total magmatic heat flux (J m^{-2}); L is the latent heat of crystallisation (J kg^{-1}); C_p is the specific heat capacity of the basalt (J kg^{-1} K^{-1}); and ΔT is the axial change in temperature of the cooling basalt (°C).

The axial magmatic heat flux available to drive high temperature hydrothermal circulation is taken as that associated with crystallisation and cooling of the sheeted dike complex and the lower crust, given that the great majority of the lower crust must form close to the axis in order to develop the observed prominent Moho seismic reflector and transmit shear waves. In addition to the latent heat (5×10^5 J kg^{-1}, Table 1; Ghiorso and Sack, 1995; Kojitani and Akaogi, 1997), close to the ridge axis the lower crust must cool to subsolidus temperatures of less than 1000 °C releasing 1085 J kg^{-1} K^{-1} of specific heat. At Site 1256 the total crustal thickness is 5.0–5.5 km (Wilson et al., 2003) of which the lower crust accounts for 3.75–4.25 km, given the drilled upper crustal thickness of 1.25 km above the dike/gabbro transition. Assuming a density of 2.9×10^3 kg m^{-3} (Blackman et al., 2006) for the lower crust, $7.3–8.3 \times 10^{12}$ J m^{-2} of heat is released from crystallising and cooling a 1 m^2 column of lower crust of this thickness to 1000 °C. Crystallising and cooling the sheeted dike complex releases an additional 1.4×10^6 J kg^{-1}. The total heat released from forming both the sheeted dikes (0.4 km) and the lower crust (3.75–4.25 km) at Hole 1256D is $9.5–10.6 \times 10^{12}$ J m^{-2}. Further cooling of the lower crust below 1000 °C would increase this heat flux.

Our estimate of the heat transported by fluid flow through the Site 1256 upper crust ($2.9–6.2 \times 10^{12}$ J m^{-2}) is significantly less than the total heat released during formation of the sheeted dikes and the lower crust ($9.5–10.6 \times 10^{12}$ J m^{-2}). Consequently, the upper crustal hydrothermal system can only account for removal of up to 29–61% of the total heat that must be removed to cool and crystallise the crust at Site 1256 (Fig. 7), based on the assertion that the lower crust will lose a only small proportion of the heat flux via conductive cooling (<10%; e.g., Phipps Morgan and Chen, 1993). This requires additional hydrothermal circulation at Site 1256 that is not recorded by the sampled sheeted dikes,

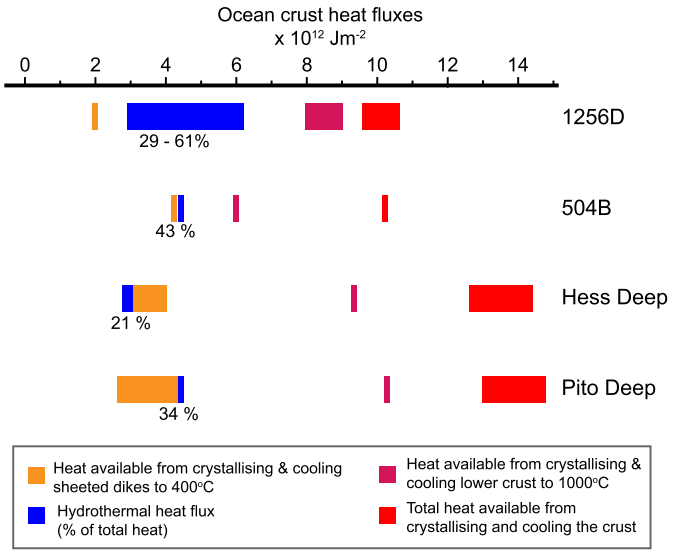

Fig. 7. Time-integrated fluid fluxes and heat fluxes for each of the crustal study sites, showing the percentage of heat available from the crystallisation and cooling of the sheeted dikes and lower crust that is removed by the upper crustal hydrothermal system. Data presented in this figure is located in Supplementary Material Table 2.

but that is equal to or greater than that currently recorded by the sheeted dike complex. Other study sites produce similar estimates for the total heat removed by the upper crustal hydrothermal system (21–42%, Fig. 7; Barker et al., 2008) suggesting the observations from Hole 1256D are representative of fast to intermediate spreading rate crust.

5.4. Deep hydrothermal circulation

Our results require that extensive hydrothermal fluid–rock exchange must occur elsewhere in the crust to remove the remaining heat from the lower crust and satisfy the geophysical observations that the lower crust is fully crystallised and cooled to $<1000\,^{\circ}C$ within a few km of the ridge axis. Recent thermal models suggest that deep hydrothermal circulation may occur in the lower crust if it is sufficiently permeable (Theissen-Krah et al., 2016). We propose two possible scenarios for the geometry of this hydrothermal system that are thermally viable to make predictions of the anticipated $^{87}Sr/^{86}Sr$ profile of Hole 1256D when it is extended into cumulate gabbros: (1) a larger upper crustal hydrothermal system that extends down into the lower crust; and (2) the presence of a separate hydrothermal system in the lower crust for which recharge fluids have by-passed reaction with the sheeted dikes (Fig. 8).

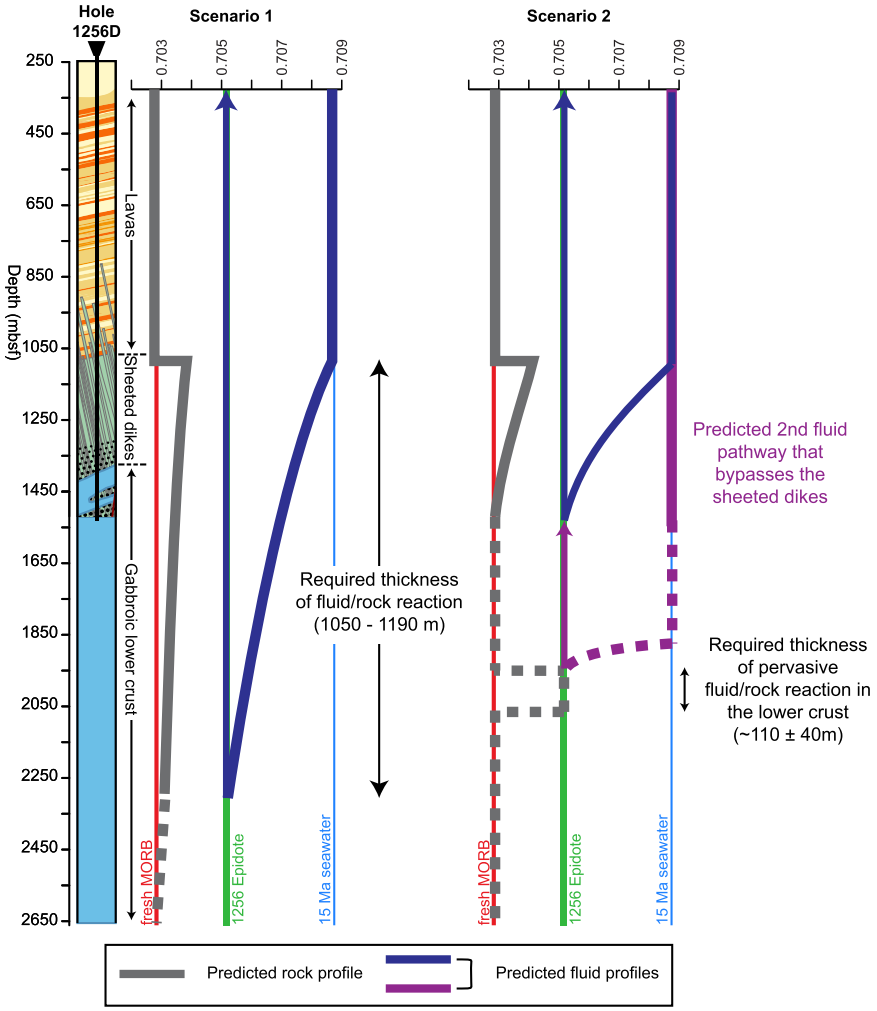

Fig. 8. Illustrations of the proposed geometries of the hydrothermal system in the lower crust for scenarios 1 and 2, showing the predicted $^{87}Sr/^{86}Sr$ evolution of both the fluid and rock. In scenario 1, the upper crustal hydrothermal system penetrates down into the lower crust as the CBL migrates downwards. Scenario 2 represents a hydrothermal system that has not reacted with the upper crust before reaching the lower crust. Both of these scenarios could remove the necessary heat flux from crystallising and cooling the lower crust.

Scenario 1 implies that the existing hydrothermal system in the sheeted dikes represents only the uppermost portion of a larger continuous hydrothermal system that has penetrated deeper into the gabbros in response to a downward migrating CBL. The tracer transport method can be used to estimate the total depth of this hydrothermal system by using the total fluid flux necessary to extract all of the available heat from the crust. The total hydrothermal fluid flux (heating the fluid to ~440 °C, following section 5.3.1) needed for Hole 1256D is 5.0–5.4 $\times 10^6$ kg m^{-2}. Using the previous constraints (Section 3), the tracer transport model is iteratively solved by increasing the depth of the model until the required hydrothermal fluid flux is achieved. For Hole 1256D the total required depth for the hydrothermal system is 1050–1190 m, indicating that fluid circulation must penetrate a further 660 to 800 m into the gabbros (Fig. 8).

Scenario 2 proposes the existence of an additional hydrothermal system in the lower crust, and critically, that fluid recharge has bypassed fluid/rock reaction with the sheeted dikes sampled in Hole 1256D. This could be achieved by focused fluid flow through the upper crust, perhaps along faults (Coogan et al., 2006) or in a restricted downwelling zone (Fig. 8; Tolstoy et al., 2008). The size of this hydrothermal system can be estimated from the total heat flux available, the upper crustal heat flux that is removed, and by considering the potential temperature of fluids in the lower crust. The distribution of this fluid flux in the lower crust and the extent of fluid/rock exchange are highly speculative. As a starting point we consider the minimum amount of lower crust that would have to be in equilibrium with the hydrothermal fluid in order to account for the heat flux deficit, assuming the fluid entered the lower crust as cold seawater and evolved into hydrothermal fluids with compositions comparable to those in the sheeted dike complex. For a direct comparison to the upper crust, if the fluid reaches ~440 °C (following section 5.3.1), 69–150 m of lower crust would need to be in equilibrium with the hydrothermal fluid. If the fluid was heated to ~470 °C at 500 bar (a more realistic pressure, heat required = 2.1 $\times 10^6$ J kg^{-1}, Driesner, 2007), it would be recorded as 66–139 m of lower crust in Sr-isotopic equilibrium with the hydrothermal fluid (Fig. 8).

The lower crust has been sampled at tectonic windows and ophiolites and these provide some insight into the potential lower crustal hydrothermal system and the viability of the two scenarios suggested for Hole 1256D. The uppermost (800 m) lower crust sampled at Hess Deep comprises pervasively altered gabbroic rocks with lateral variability in mineral assemblages from amphibolite to greenschist facies (Kirchner and Gillis, 2012), reminiscent of our Scenario 1. Mg-in-plagioclase cooling rate estimates for the uppermost gabbros suggest rapid cooling rates (0.01–0.1 °C/yr) commensurate with intense hydrothermal cooling (Faak et al., 2015). However, whole rock $^{87}Sr/^{86}Sr$ are only slightly elevated relative to MORB indicating these gabbros have undergone minor fluid/rock reaction, similar to the central portions of the gabbroic intrusions sampled in Hole 1256D that exhibit only minor Sr isotope exchange (Harris et al., 2015). Tonalite samples from Hess Deep do have elevated Sr isotope compositions (0.7038) compared to the host gabbro, as observed in Hole 1256D. However, no zones of extensive Sr isotope exchange are recorded in the gabbroic rocks from Hess Deep, in contrast to Hole 1256D, where restricted zones associated with igneous contacts yield Sr-isotope ratios similar to the proposed hydrothermal end member (Harris et al., 2015) and appear to be fluid conduits. Kirchner and Gillis (2012) consider the uppermost plutonics to form part of the upper crustal hydrothermal system (similar to scenario 1) and calculate a fluid flux of 2.1–2.5 $\times 10^6$ kg m^{-2}. However, this is insufficient to remove the heat available from the lower crust, and requires additional hydrothermal cooling. For scenario 1 to be valid we predict that the Sr-isotopic compositions of the upper ~700–800 m of gabbros at Site 1256 will be strongly altered towards our estimated hydrothermal fluid ($^{87}Sr/^{86}Sr$ ~0.705). If this is not observed, some focused fluid recharge must bypass the sheeted dike complex (scenario 2).

Evidence for focused fluid flow in the lower crust, like that proposed for scenario 2, has been observed in the Semail ophiolite in Oman where 10–50 m-wide alteration zones occur at ~1 km spacings in gabbros (Coogan et al., 2006). These zones are associated with strong hydrothermal alteration, high vein intensities and record fluid–rock exchange and mineral precipitation from amphibolite down to lower greenschist facies conditions (Coogan et al., 2006). The estimated fluid flux through these focused zones are an order of magnitude greater than the fluid flux through the Oman sheeted dike complex. If present, such features could account for the lower crust heat flux deficit apparent in Hole 1256D, assuming that the hydrothermal alteration of Semail ophiolite is an appropriate analogue for fast spreading ocean crust. We would predict that a deepened Hole 1256D may encounter 10–100 m-wide isolated zones of hydrothermally altered gabbros with strongly elevated Sr-isotope compositions. The uppermost kilometre of the lower crust therefore represents a critical region for assessing the hydrothermal, igneous and structural observations that will allow the end member models for the lower crust to be robustly tested.

6. Summary and conclusions

The Sr-isotope profile through the sheeted dikes at ODP Site 1256 is significantly different from those previously sampled in Hole 504B and the Hess Deep and Pito Deep tectonic windows (Harris et al., 2015). In contrast to the MORB-like profiles from these latter three sections, the $^{87}Sr/^{86}Sr$ of the dikes in Hole 1256D are strongly elevated from MORB values (~0.7028) towards the estimated composition of the Site 1256 black smoke-type hydrothermal fluid (~0.705), indicating a much greater extent of fluid–rock Sr-isotope exchange (Fig. 5). We have applied tracer transport mass balance to the high density $^{87}Sr/^{86}Sr$ profile of the Hole 1256D sheeted dike complex to quantify the high temperature axial fluid flux resulting from pervasive fluid recharge through the sheeted dikes to be 1.5–3.2 $\times 10^6$ kg m^{-2}. Despite the different extents of Sr-isotope exchange, given the different thicknesses of the sheeted dike complexes (Hole 1256D ~400 m; Hess, ~600 m; 504B, Pito ~1000 m), the time-integrated fluid flux through Hole 1256D is similar to those estimated from the other sites (Teagle et al., 2003; Barker et al., 2008), and estimates using alternative geochemical tracers (e.g., Li, Tl, S). This suggests that the axial recharge flux through the sheeted dikes is remarkably uniform at intermediate to superfast spreading rates.

This estimate of high temperature upper crustal hydrothermal fluid flux is sufficient to remove only 29–61% of the sensible and latent heat released during crystallisation and cooling of the Site 1256 lower crust, and requires deeper hydrothermal circulation in the lower crust to satisfy the geophysical observations of modern mid-ocean ridges. Two scenarios are suggested, that can be tested by further drilling in Hole 1256D: (1) that the extensive hydrothermal alteration observed in the sheeted dikes continues for up to 800 m into the underlying upper gabbros, or that (2) a significant portion of fluid recharge (~50%) bypasses the sheeted dikes by focused fluid flow on faults or in discrete zones, and reaction with these fluids should produce 10–100 m-wide isolated zones of hydrothermally altered gabbros with strongly elevated Sr-isotope compositions, as are seen in some ophiolites.

Acknowledgements

This research used samples and data provided by the Ocean Drilling Program and the Integrated Ocean Drilling Program. We

gratefully acknowledge reviews from A. Barker and K. Gillis and comments from the editor that improved this manuscript. This research was funded by NERC grants NER/T/S/2003/00048 and NE/E001971/1 to DAHT, NERC studentships to MH (NER/S/A/2005/13475A), post-cruise funding to MH (NE/L00059/1; IODP Exp 335), rapid response funding from UK-IODP to DAHT, RMC, CSD and MH (ODP 206, IODP Exp. 309/312, 335) and Engineering and Physical Science Research Council Doctoral Training Centre grant EP/G03690X/1 (MCW). DAHT acknowledges a Royal Society Wolfson Foundation Merit Award (WM130051) that supported this research.

Appendix A. Supplementary material

Supplementary material related to this article can be found online at http://dx.doi.org/10.1016/j.epsl.2017.01.010.

References

Alt, J.C., Laverne, C., Vanko, D.A., Tartarotti, P., Teagle, D.A.H., Bach, W., Zuleger, E., Erzinger, J., Honnorez, J., Pezard, P.A., Becker, K., Salisbury, M.H., Wilkens, R.H., 1996. Hydrothermal alteration of a section of upper oceanic crust in the Eastern Equatorial Pacific: a synthesis of results from site 504 (DSDP legs 69, 70 and 83, and ODP legs 111, 137, 140 and 148). In: Alt, J.C., Kinoshita, H., Stokking, L.B., Michael, P.J. (Eds.), Proc. Ocean Drill. Program Sci. Results, vol. 148, pp. 417–434.

Alt, J.C., Laverne, C., Coggon, R.M., Teagle, D.A.H., Banerjee, N.R., Morgan, S., Smith-Duque, C.E., Harris, M., Galli, L., 2010. Subsurface structure of a submarine hydrothermal system in ocean crust formed at the East Pacific Rise, ODP/IODP Site 1256. Geochem. Geophys. Geosyst. 11, Q10010.

Bach, W., Humphris, S.E., 1999. Relationship between the Sr and O isotope compositions of hydrothermal fluids and the spreading and magma-supply rates at oceanic spreading centers. Geology 27, 1067–1070.

Baker, E.T., Chen, Y.J., Phipps Morgan, J., 1996. The relationship between near-axis hydrothermal cooling and the spreading rate of mid-ocean ridges. Earth Planet. Sci. Lett. 142, 137–145.

Barker, A.K., Coogan, L.A., Gillis, K.M., Weis, D., 2008. Strontium isotope constraints on fluid flow in the sheeted dike complex of fast spreading crust: pervasive fluid flow at Pito Deep. Geochem. Geophys. Geosyst. 9.

Barker, A.K., Coogan, L.A., Gillis, K.M., 2010a. Insights into the behaviour of sulphur in mid-ocean ridge axial hydrothermal systems from the composition of the sheeted dyke complex at Pito Deep. Chem. Geol. 275, 105–115.

Barker, A.K., Coogan, L.A., Gillis, K.M., Hayman, N.W., Weis, D., 2010b. Direct observation of a fossil high-temperature, fault-hosted, hydrothermal upflow zone in crust formed at the East Pacific Rise. Geology 38, 379–382.

Berman, R.G., 1998. Internally-consistent thermodynamic data for minerals in the system Na_2O–K_2O–CaO–MgO–FeO–Fe_2O_3–Al_2O_3–SiO_2–TiO_2–H_2O–CO_2. J. Petrol. 29, 445–522.

Berndt, M.E., Seyfried, W.E., Beck, J.W., 1988. Hydrothermal alteration processes at midocean ridges: experimental and theoretical constraints from Ca and Sr exchange reactions and Sr isotopic ratios. J. Geophys. Res. 93, 4573–4583.

Bickle, M.J., 1992. Transport mechanisms by fluid-flow in metamorphic rocks: oxygen and strontium decoupling in the Trois Seigneurs massif – a consequence of kinetic dispersion? Am. J. Sci. 292, 289–316.

Bickle, M.J., Teagle, D.A.H., 1992. Strontium alteration in the Troodos ophiolite: implications for fluid fluxes and geochemical transport in mid-ocean ridge hydrothermal systems. Earth Planet. Sci. Lett. 113, 219–237.

Bischoff, J.L., Rosenbauer, R.J., 1985. An equation of state for hydrothermal seawater (3.2% NaCl). Am. J. Sci. 285, 725–763.

Blackman, D.K., Ildefonse, B., John, B.E., Ohara, Y., Miller, D.J., MacLeod, C.J., Expedition 304/305 Scientists, 2006. Oceanic Core Complex Formation, Atlantis Massif.

Boudier, F., Nicolas, A., Ildefonse, B., 1996. Magma chambers in the Oman ophiolite: fed from the top or the bottom? Earth Planet. Sci. Lett. 144, 239–250.

Chan, L.-H., Alt, J.C., Teagle, D.A.H., 2002. Lithium and lithium isotope profiles through the upper oceanic crust: a study of seawater–basalt exchange at ODP Sites 504B and 896A. Earth Planet. Sci. Lett. 201, 187–201.

Coogan, L.A., 2008. Reconciling temperatures of metamorphism, fluid fluxes, and heat transport in the upper crust at intermediate to fast spreading mid-ocean ridges. Geochem. Geophys. Geosyst. 9, Q02013.

Coogan, L.A., Dosso, S., 2012. An internally consistent, probabilistic, determination of ridge-axis hydrothermal fluxes from basalt-hosted systems. Earth Planet. Sci. Lett. 323, 92–101.

Coogan, L.A., Howard, K.A., Gillis, K.M., Bickle, M.J., Chapman, H., Boyce, A.J., Jenkin, G.R.T., Wilson, R.N., 2006. Chemical and thermal constraints on focussed fluid flow in the lower oceanic crust. Am. J. Sci. 306, 389–427.

Driesner, T., 2007. The system H_2O–NaCl. Part II: correlations for molar volume, enthalpy, and isobaric heat capacity from 0 to 1000 °C, 1 to 5000 bar, and 0 to 1 XNaCl. Geochim. Cosmochim. Acta 71, 4902–4919.

Elderfield, H., Schultz, A., 1996. Mid-ocean ridge hydrothermal fluxes and the chemical composition of the ocean. Annu. Rev. Earth Planet. Sci. 24, 191–224.

Faak, K., Coogan, L.A., Chakraborty, S., 2015. Near conductive cooling rates in the upper-plutonic section of crust formed at the East Pacific Rise. Earth Planet. Sci. Lett. 423, 36–47.

France, L., Ildefonse, B., Koepke, J., 2009. Interactions between magma and hydrothermal system in Oman ophiolite and in IODP Hole 1256D: fossilization of a dynamic melt lense at fast spreading ridges. Geochem. Geophys. Geosyst. 10, Q10O19. http://dx.doi.org/10.1029/2009GC002652.

Gao, Y., Vils, F., Cooper, K.M., Banerjee, N., Harris, M., Hoefs, J., Teagle, D.A.H., Casey, J.F., Elliott, T., Laverne, C., Alt, J.C., Muehlenbachs, K., 2012. Downhole variation of lithium and oxygen isotopic compositions of oceanic crust at East Pacific Rise, ODP Site 1256. Geochem. Geophys. Geosyst. 13, Q10001.

Ghiorso, M.S., Sack, R.O., 1995. Chemical mass transfer in magmatic processes IV. A revised and internally consistent thermodynamic model for the interpolation and extrapolation of liquid-solid equilibria in magmatic systems at elevated temperatures and pressures. Contrib. Mineral. Petrol. 119, 197–212.

Gillis, K.A., Coogan, L.A., Pedersen, R., 2005. Strontium isotope constraints on fluid flow in the upper oceanic crust at the East Pacific Rise. Earth Planet. Sci. Lett. 232, 83–94.

Gillis, K.M., 2008. The roof of an axial magma chamber: a hornfelsic heat exchanger. Geology 36, 299–302.

Gillis, K.M., Coogan, L.A., 2002. Antarctic migmatites from the roof of an ocean ridge magma chamber. J. Petrol. 43, 2075–2095.

Harris, M., Coggon, R.M., Smith-Duque, C.E., Cooper, M.J., Milton, J.A., Teagle, D.A.H., 2015. Channelling of hydrothermal fluids during the accretion and evolution of the upper oceanic crust: Sr isotope evidence from ODP Hole 1256D. Earth Planet. Sci. Lett. 416, 56–66.

Heft, K.L., Gillis, K.M., Pollock, M.A., Karson, J.A., Klein, E.M., 2008. Role of upwelling hydrothermal fluids in the development of alteration patterns at fast spreading ridges: evidence from the sheeted dike complex at Pito Deep. Geochem. Geophys. Geosyst. 9, Q05007.

Henstock, T.J., Woods, A.W., White, R.S., 1993. The accretion of oceanic-crust by episodic sill intrusion. J. Geophys. Res., Solid Earth 98, 4143–4161.

Kelemen, P.B., Koga, K., Shimizu, N., 1997. Geochemistry of gabbro sills in the crust-mantle transition zone of the Oman ophiolite: implications for the origin of the oceanic lower crust. Earth Planet. Sci. Lett. 146, 475–488.

Kelemen, P.B., Manning, C.E., 2015. Reevaluating carbon fluxes in subduction zones, what goes down, mostly comes up. Proc. Natl. Acad. Sci. 112, 3997–4006.

Kirchner, T.M., Gillis, K.M., 2012. Mineralogical and strontium isotopic record of hydrothermal processes in the lower ocean crust at and near the East Pacific Rise. Contrib. Mineral. Petrol. 164, 123–141.

Koepke, J., Christie, D.M., Dziony, W., Holtz, F., Lattard, D., Maclennan, J., Park, S., Scheibner, B., Yamasaki, T., Yamazaki, S., 2008. Petrography of the dike–gabbro transition at IODP Site 1256 (equatorial Pacific): the evolution of the granoblastic dikes. Geochem. Geophys. Geosyst. 9, Q07O09.

Kojitani, H., Akaogi, M., 1997. Melting enthalpies of mantle peridotite: calorimetric determinations in the system CaO–MgO–Al_2O_3–SiO_2 and application to magma generation. Earth Planet. Sci. Lett. 153, 209–222.

MacLeod, C.J., Yoauancq, G., 2000. A fossil melt lens in the Oman ophiolite: implications for magma chamber processes at fast spreading ridges. Earth Planet. Sci. Lett. 176, 357–373.

McArthur, J.M., Howarth, R.J., Bailey, T.R., 2001. Strontium isotope stratigraphy: LOWESS version 3: best fit to the marine Sr-isotope curve for 0–509 Ma and accompanying look-up table for deriving numerical age. J. Geol. 109, 155–170.

Morton, J.L., Sleep, N.H., 1985. A mid-ocean ridge thermal model: constraints on the volume of axial hydrothermal heat flux. J. Geophys. Res. 90, 11345–11354.

Nielson, S.G., Rehkamper, M., Teagle, D.A.H., Butterfield, D.A., Alt, J.C., Halliday, A.N., 2006. Hydrothermal fluid fluxes calculated from the isotopic mass balance of thallium in the oceanic crust. Earth Planet. Sci. Lett. 251, 120–133.

Palmer, M.R., Edmond, J.M., 1989. The strontium isotope budget of the modern ocean. Earth Planet. Sci. Lett. 92, 11–26.

Phipps Morgan, J., Chen, Y.J., 1993. The genesis of oceanic crust: magma injection, hydrothermal circulation and crustal flow. J. Geophys. Res. 98, 6283–6297.

Press, W.H., Teukolsky, S.A., Vetterling, W.T., Flannery, B.P., 1992. Numerical Recipes in C: The Art of Scientific Computing, 2nd ed. Cambridge University Press, Cambridge.

Quick, J.E., Denlinger, R.P., 1993. Ductile deformation and the origin of layered gabbro in ophiolites. J. Geophys. Res. 98, 14015–14027.

Rutter, J.E., 2015. Characterising Low Temperature Alteration and Oxidation of the Upper Oceanic Crust. Faculty of Natural and Environmental Sciences, Ocean and Earth Science, University of Southampton, p. 353.

Sano, T., Miyoshi, M., Ingle, S., Banerjee, N.R., Ishimoto, M., Fukuoka, T., 2008. Boron and chlorine contents of upper oceanic crust: basement samples from IODP Hole 1256D. Geochem. Geophys. Geosyst. 9, Q12015.

Stein, C.A., Stein, S., 1994. Constraints on hydrothermal heat flux through the oceanic lithosphere from global heat flow. J. Geophys. Res. 99, 3081–3095.

Teagle, D.A.H., Alt, J.C., Halliday, A.N., 1998. Tracing the chemical evolution of fluids during hydrothermal recharge: constraints from anhydrite recovered in ODP Hole 504B. Earth Planet. Sci. Lett. 155, 167–182.

Teagle, D.A.H., Bickle, M.J., Alt, J.C., 2003. Recharge flux to ocean-ridge black smoker systems: a geochemical estimate from ODP Hole 504B. Earth Planet. Sci. Lett. 210, 81–89.

Teagle, D.A.H., Alt, J.C., Umino, S., Miyashita, S., Banerjee, N.R., Wilson, D.S., et al., 2006. Superfast Spreading Rate Crust 2 and 3. In: Proceedings of the Integrated Ocean Drilling Program. IODP-MI Inc., Washington, DC.

Teagle, D.A.H., Ildefonse, B., Blum, P., et al., 2012. Superfast Spreading Rate Crust 4, Proceedings of the Integrated Ocean Drilling Program. In: Proceedings of the Integrated Ocean Drilling Program. IODP-MI Inc., Tokyo.

Theissen-Krah, S., Rüpke, L.H., Hasenclever, J., 2016. Modes of crustal accretion and their implications for hydrothermal circulation. Geophys. Res. Lett., 2015GL067335.

Tolstoy, M., Waldhauser, F., Bohnenstiehl, D.R., Weekly, R.T., Kim, W.-Y., 2008. Seismic identification of along-axis hydrothermal flow on the East Pacific Rise. Nature 451, 181–184.

Von Damm, K.L., 1995. Controls on the Chemistry and Temporal Variability of Seafloor Hydrothermal Fluids. Geophysical Monograph.

Wilson, D.S., 1996. Fastest known spreading on the Miocene Cocos–Pacific plate boundary. Geophys. Res. Lett. 23, 3003–3006.

Wilson, D.S., Teagle, D.A.H., Acton, G.D., et al., 2003. An in situ section of upper oceanic crust formed by superfast seafloor spreading. In: Proc. Ocean Drill. Program, Initial Rep. ODP, College Station, TX.

Wilson, D.S., Teagle, D.A.H., Alt, J.C., Banerjee, N.R., Umino, S., Miyashita, S., Acton, G.D., Anma, R., Barr, S.R., Belghoul, A., Carlut, J., Christie, D.M., Coggon, R.M., Cooper, K.M., Cordier, C., Crispini, L., Durand, S.R., Einaudi, F., Galli, L., Gao, Y., Geldmacher, J., Gilbert, L.A., Hayman, N.W., Herrero-Bervera, E., Hirano, N., Holter, S., Ingle, S., Jiang, S., Kalberkamp, U., Kerneklian, M., Koepke, J., Laverne, C., Vasquez, H.L.L., Maclennan, J., Morgan, S., Neo, N., Nichols, H.J., Park, S.-H., Reichow, M.K., Sakuyama, T., Sano, T., Sandwell, R., Scheibner, B., Smith-Duque, C.E., Swift, S.A., Tartarotti, P., Tikku, A.A., Tominaga, M., Veloso, E.A., Yamasaki, T., Yamazaki, S., Ziegler, C., 2006. Drilling to gabbro in intact ocean crust. Science 312, 1016–1020.